

## Multistep processes in the $^{12}\text{C}(^6\text{Li},d)$ stripping reaction

N. Keeley,<sup>\*</sup> T. L. Drummer,<sup>†</sup> and E. E. Bartosz<sup>‡</sup>

*Department of Physics, The Florida State University, Tallahassee, Florida 32306-4350*

C. R. Brune<sup>§</sup>

*Department of Physics and Astronomy, University of North Carolina at Chapel Hill, Chapel Hill, North Carolina 27599-3255  
and Triangle Universities Nuclear Laboratory, Durham, North Carolina 27088-0308*

P. D. Cathers<sup>||</sup>

*Department of Physics, The Florida State University, Tallahassee, Florida 32306-4350*

M. Fauerbach<sup>¶</sup>

*Department of Physics, The Florida State University, Tallahassee, Florida 32306-4350*

H. J. Karwowski

*Department of Physics and Astronomy, University of North Carolina at Chapel Hill, Chapel Hill, North Carolina 27599-3255  
and Triangle Universities Nuclear Laboratory, Durham, North Carolina 27088-0308*

K. W. Kemper

*Department of Physics, The Florida State University, Tallahassee, Florida 32306-4350*

B. Kozłowska

*Department of Physics and Astronomy, University of North Carolina at Chapel Hill, Chapel Hill, North Carolina 27599-3255;  
Triangle Universities Nuclear Laboratory, Durham, North Carolina 27088-0308;  
and Institute of Physics, University of Silesia, ul. Uniwersytecka 4, 40-007 Katowice, Poland*

E. J. Ludwig

*Department of Physics and Astronomy, University of North Carolina at Chapel Hill, Chapel Hill, North Carolina 27599-3255  
and Triangle Universities Nuclear Laboratory, Durham, North Carolina 27088-0308*

F. Maréchal<sup>\*\*</sup>

*Department of Physics, The Florida State University, Tallahassee, Florida 32306-4350*

A. J. Mendez<sup>††</sup>

*Department of Physics and Astronomy, University of North Carolina at Chapel Hill, Chapel Hill, North Carolina 27599-3255  
and Triangle Universities Nuclear Laboratory, Durham, North Carolina 27088-0308*

E. G. Myers and D. Robson

*Department of Physics, The Florida State University, Tallahassee, Florida 32306-4350*

K. Rusek

*The Andrzej Sołtan Institute for Nuclear Studies, ul. Hoża 69, 00-681 Warsaw, Poland*

K. D. Veal<sup>‡‡</sup>

*Department of Physics and Astronomy, University of North Carolina at Chapel Hill, Chapel Hill, North Carolina 27599-3255  
and Triangle Universities Nuclear Laboratory, Durham, North Carolina 27088-0308*

(Received 11 December 2002; published 18 April 2003)

The results of extensive coupled-reaction-channel calculations are compared with the cross section and new analyzing power data for the  $^{12}\text{C}(^6\text{Li},d)^{16}\text{O}$  reaction leading to the 0.0-MeV  $0^+$ , 6.13-MeV  $3^-$ , 6.92-MeV  $2^+$ , 8.87-MeV  $2^-$ , and 10.35-MeV  $4^+$  states of  $^{16}\text{O}$  at  $^6\text{Li}$  bombarding energies of 34 and 50 MeV. All the analyzing power data at both energies and all the cross section data at 50 MeV, with the exception of that for the  $^{12}\text{C}(^6\text{Li},d)^{16}\text{O}$  transition to the 0.0-MeV  $0^+$  state of  $^{16}\text{O}$  are presented here for the first time. These results suggest that there are significant multistep contributions to transfers leading to the  $0^+$  and  $3^-$  states, while those leading to the  $2^+$  and  $4^+$  states may be reasonably well described by simple direct  $\alpha$  transfer. The importance of multistep effects is found to increase with increasing bombarding energy.

DOI: 10.1103/PhysRevC.67.044604

PACS number(s): 25.70.Hi, 24.10.Eq, 21.60.Gx

## I. INTRODUCTION

For almost thirty years there has been considerable speculation about the contribution of multistep transfer processes to the population of individual states in  $^{16}\text{O}$  via the  $^{12}\text{C}(^6\text{Li},d)$  reaction [1–4], although to date no calculation has been published which attempts to quantify their presence. In fact, previous discussions only focused on transfers from excited states of the target, whereas these may also occur from “excited states” of the projectile (the three  $L=2$  resonances in  $^6\text{Li}$ ). Also, the importance of transitions between states of  $^{16}\text{O}$  has so far not been investigated. The question of the contribution of such multistep processes is an important one if the  $(^6\text{Li},d)$  reaction is ever to be used to determine  $\alpha$  spectroscopic factors. Previous attempts to extract these factors from distorted-wave Born approximation (DWBA) studies [5–8] have assumed that the reaction mechanism is dominated by direct  $\alpha$  transfer. Compound nucleus contributions were assumed to be small at forward angles for most of the low-lying states in  $^{16}\text{O}$  populated by the  $^{12}\text{C}(^6\text{Li},d)$  reaction at energies well above the Coulomb barrier. This assumption was based on the results of Hauser-Feshbach calculations of the compound nucleus component normalized to the cross section for formation of the unnatural parity 8.87-MeV  $2^-$  state, assumed to be populated purely by compound nucleus formation [5–7].

The interest in obtaining  $\alpha$  spectroscopic factors for the  $^{16}\text{O}/^{12}\text{C}$  overlap goes beyond that of probing the  $\alpha$ -clustering character of states in  $^{16}\text{O}$ . The  $^{12}\text{C}(\alpha,\gamma)^{16}\text{O}$  reaction rate is of vital importance in nuclear astrophysics, but is still relatively poorly determined [9] due to the difficulty of the measurement at astrophysically relevant energies. The  $^{12}\text{C}(^6\text{Li},d)^{16}\text{O}$  reaction may be used instead to determine the reduced  $\alpha$  widths of states in  $^{16}\text{O}$  [5]. However, an accurate determination of these reduced widths from DWBA calculations is dependent on the reaction proceeding via direct  $\alpha$  transfer. Also, the use of the asymptotic normalization coefficient method (see, e.g., Ref. [10]) for a given reaction relies on the validity of the DWBA formalism as applied to that reaction, as pointed out by Nunes and Mukhamedzhanov [11]. Thus, it is of considerable importance to determine the significance of nondirect (either mul-

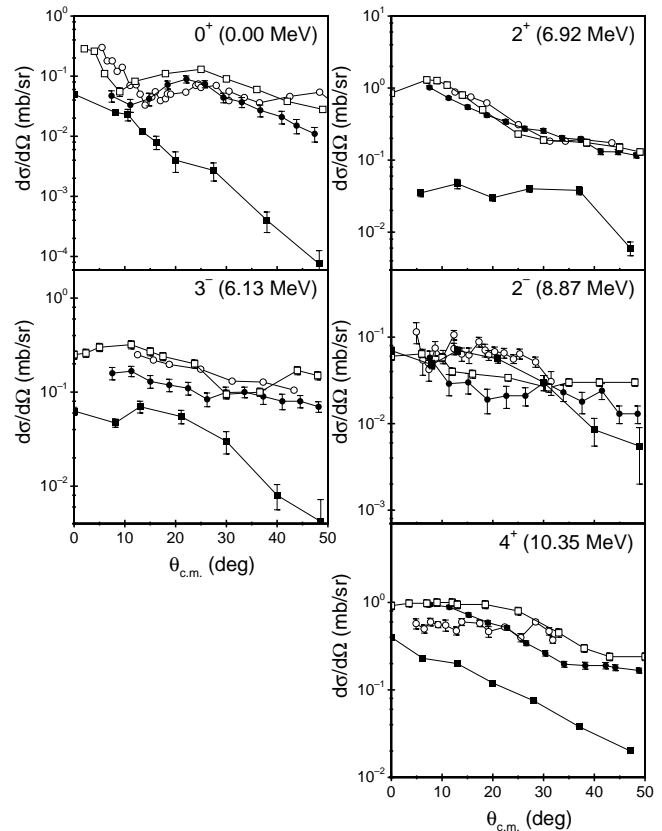


FIG. 1. Comparison of angular distributions for the  $^{12}\text{C}(^6\text{Li},d)^{16}\text{O}$  transfer reaction leading to the 0.0-MeV  $0^+$ , 6.13-MeV  $3^-$ , 6.92-MeV  $2^+$ , 8.87-MeV  $2^-$ , and 10.35-MeV  $4^+$  states in  $^{16}\text{O}$  at several different  $^6\text{Li}$  bombarding energies. The open circles denote the current 34-MeV data together with that of Cunsolo *et al.* [7], the filled circles the current 50-MeV data, the open squares the 42-MeV data of Becchetti *et al.* [5], and the filled squares the 90-MeV data of Becchetti *et al.* [6]. The lines are to guide the eye.

tistep or compound nucleus) contributions to the  $^{12}\text{C}(^6\text{Li},d)^{16}\text{O}$  reaction.

In Fig. 1 we show the present data for the  $^{12}\text{C}(^6\text{Li},d)^{16}\text{O}$  reaction leading to the 0.0-MeV  $0^+$ , 6.13-MeV  $3^-$ , 6.92-MeV  $2^+$ , 8.87-MeV  $2^-$ , and 10.35-MeV  $4^+$  states in  $^{16}\text{O}$ , measured at  $^6\text{Li}$  bombarding energies of 34 and 50 MeV together with data from the literature for the same reactions at  $^6\text{Li}$  bombarding energies of 34 MeV [7], 42 MeV [5], and 90 MeV [6]. Note that while the 34-, 42-, and 50-MeV cross sections are of similar magnitudes and have similar shapes as a function of angle, the 90-MeV cross sections (with the exception of the 8.87-MeV  $2^-$  state) are all of considerably smaller magnitude.

In this work we present for the first time the results of extensive coupled-reaction-channel (CRC) calculations including several multistep paths for the  $^{12}\text{C}(^6\text{Li},d)^{16}\text{O}$  reaction leading to the 0.0-MeV  $0^+$ , 6.13-MeV  $3^-$ , 6.92-MeV  $2^+$ , 8.87-MeV  $2^-$ , and 10.35-MeV  $4^+$  states of  $^{16}\text{O}$ , which are compared with new analyzing power data for  $^6\text{Li}$  at bombarding energies of 34 and 50 MeV and a combination of new and previously measured [7] cross section data. The

\*Email address: keeley@nucmar.physics.fsu.edu

†Present address: University of Illinois, Urbana, Illinois.

‡Present address: CyTerra Corporation, Orlando, Florida.

§Present address: Department of Physics and Astronomy, Ohio University, Athens, Ohio.

||Present address: University of Belize, Belize City, Belize.

¶Present address: Florida Gulf Coast University, Fort Myers, Florida.

\*\*Present address: Institut de Recherches Subatomiques, Strasbourg, France.

††Present address: Oak Ridge National Laboratory, Oak Ridge, Tennessee.

‡‡Present address: Los Alamos National Laboratory, Los Alamos, New Mexico.

cross section and analyzing powers for the  $^{12}\text{C}(^6\text{Li},d)^{16}\text{O}$  transition to the 0.0-MeV  $0^+$  state of  $^{16}\text{O}$  for 50-MeV  $^6\text{Li}$  have been previously published [8]. All other analyzing power data at both energies and cross section data at 50 MeV are presented here for the first time. We have confined our analysis to the strongly populated states in  $^{16}\text{O}$  for which we were able to obtain angular distributions of the analyzing powers. Section II of the present work provides a description of the experimental procedure, while Sec. III summarizes the results of previous DWBA calculations. The current CRC calculations are described in Sec. IV and the results discussed in Sec. V. Our conclusions are presented in Sec. VI.

## II. EXPERIMENTAL PROCEDURE

The present  $^{12}\text{C}(^6\text{Li},d)$  cross section and analyzing power data at 34 and 50 MeV were measured with similar experimental procedures. Polarized  $^6\text{Li}$  beams were produced by the Florida State University (FSU) optically pumped polarized lithium ion source [12] and accelerated to 34 MeV by the FSU FN tandem van de Graaff accelerator. For the higher energy measurements, the 34-MeV beam was injected into a superconducting linear accelerator that accelerated the beam to 50 MeV. The  $(^6\text{Li},d)$  analyzing powers were measured using a large scattering chamber containing a 200 (500)  $\mu\text{g}/\text{cm}^2$  self-supporting natural carbon target for  $^6\text{Li}$  beam energies of 34 (50) MeV, followed by a smaller chamber filled with He gas at a pressure of 600 Torr, used to monitor the beam polarization and separated from the main chamber by a thin Havar foil.

Four Si surface-barrier detector telescopes (two on each side of the beam) in the main chamber measured the  $(^6\text{Li},d)$  analyzing powers, while two single Si surface-barrier detectors (one on each side of the beam) in the He-filled polarimeter chamber monitored the  $^6\text{Li}$  beam polarization by detecting the  $^4\text{He}$  recoil particles at detector angles between  $13^\circ$  and  $21^\circ$ . The yields from these detectors were also used to determine the absolute beam polarization using previously established standards [13]. Typical absolute beam polarizations were  $|t_{10}| = 0.96 \pm 0.03$  and  $t_{20} = -1.02 \pm 0.030$ . A thin Ta foil was placed in front of the detector telescopes in the main chamber to stop the intense elastically scattered beam particles from damaging the detectors during the long times needed to determine the reaction analyzing powers. Cross section angular distributions were obtained using an unpolarized  $^6\text{Li}$  beam produced by a standard sputter ion source.

In the present work, the 6.05-MeV  $0^+$  and 7.12-MeV  $1^-$  states of  $^{16}\text{O}$  could not be resolved from the nearby 6.13-MeV  $3^-$  and 6.92-MeV  $2^+$  states, respectively. However, the high resolution 42-MeV data of Becchetti *et al.* [5] contains angular distributions for both the 6.05-MeV  $0^+$  and 7.12-MeV  $1^-$  states. These data indicate that the 7.12-MeV  $1^-$  state cross section is  $\approx 10\%$  of that for the 6.92-MeV  $2^+$  state, so the unresolved  $2^+ + 1^-$  data was analyzed as a pure  $2^+$  state. The 6.05-MeV  $0^+$  angular distribution is highly oscillatory and gives a contribution of about 25% to the 6.13-MeV  $3^-$  state data in the angular range between  $20^\circ$  and  $40^\circ$ . With the aid of finite-range DWBA calculations [14], it

was possible to remove the contribution of this state from the combined  $3^- + 0^+$  data. To extract the  $0^+$  state contribution from the measured combined vector analyzing power  $iT_{11}$ , the calculated  $0^+$   $iT_{11}$  was subtracted using the following expression:

$$iT_{11}^{3^-}(\text{corrected}) = \left(1 - \frac{\sigma(0^+)}{\sigma(3^- + 0^+)}\right) iT_{11}^{3^-} - \left(1 - \frac{\sigma(0^+)}{\sigma(3^- + 0^+)}\right) iT_{11}^{0^+}, \quad (1)$$

where  $\sigma(0^+)$  is the calculated  $0^+$  cross section and  $\sigma(3^- + 0^+)$  is the measured combined  $3^- + 0^+$  cross section. The measured vector analyzing power for the uncorrected  $3^-$  state (which includes  $0^+$  contributions) is denoted by  $iT_{11}^{3^-}$ , while  $iT_{11}^{0^+}$  denotes the calculated  $0^+$  vector analyzing power. Errors were obtained by propagating the errors of the individual quantities, with values of 10% assumed for the calculated quantities. The tensor analyzing powers,  $T_{20}$ ,  $T_{21}$ , and  $T_{22}$  were not separated as the calculated  $0^+$  tensor analyzing powers were close to zero at all angles.

## III. SUMMARY OF PREVIOUS DWBA ANALYSES

There are a number of DWBA analyses of the  $^{12}\text{C}(^6\text{Li},d)^{16}\text{O}$  reaction at various energies in the literature. However, many of these are mainly concerned with comparing different formulations of finite-range DWBA, and thus only compare calculations with data for transfer to a single state in  $^{16}\text{O}$ . The first comparison of finite-range DWBA calculations with an extensive set of data for the  $^{12}\text{C}(^6\text{Li},d)^{16}\text{O}$  reaction that we are aware of is that of Becchetti *et al.* [5] for a  $^6\text{Li}$  bombarding energy of 42 MeV. The fits to the 0.0-MeV  $0^+$ , 6.13-MeV  $3^-$ , 6.92-MeV  $2^+$ , and 10.35-MeV  $4^+$  states of  $^{16}\text{O}$  are comparable to those presented below with the exception of the  $2^+$  state, where the calculated angular distribution peaks at an angle larger than the measured one.

Finite-range DWBA calculations are compared with data at  $^6\text{Li}$  bombarding energies of 28 and 34 MeV by Cunsolo *et al.* [7]. Again, fits are comparable to those presented below, with the fit to the 10.35-MeV  $4^+$  state for the 34-MeV incident  $^6\text{Li}$  being considerably better than that obtained here. Apagyí and Vertse [15] present comparisons of zero-range DWBA using microscopic form factors with data at 18 and 20 MeV. The agreement is poor in almost all cases.

Finite-range DWBA calculations are compared with data at 90 MeV by Becchetti *et al.* [6]. Again, the fits to the data are of comparable quality to those presented below, depending on the choice of optical model potentials used.

Insolia *et al.* [16] compared zero-range DWBA calculations using microscopic four-particle transfer form factors with data at 28 and 34 MeV. The agreement is comparable to that obtained with the current calculations.

Mention must also be made of the work of Makowska-Rzeszutko *et al.* [17]. Although these authors compare finite-range DWBA to data for transfer to the  $^{16}\text{O}$  ground state

TABLE I. Number of radial nodes  $N$  and spectroscopic amplitudes for the  $^{12}\text{C}/^{16}\text{O}$  overlaps used in the present calculations. The number of radial nodes includes that at the origin but excludes that at infinity. The spin of the final state in  $^{16}\text{O}$  is denoted by  $J$ ,  $I$  denotes the spin of the  $^{12}\text{C}$  core, and  $L$  the  $\alpha$ - $^{12}\text{C}$  relative angular momentum.

$J$	$E_x$ (MeV)	Channel ( $I,L$ )					
		(0, $J$ )	(2, $J-2$ )	(2, $J-1$ )	(2, $J$ )	(2, $J+1$ )	(2, $J+2$ )
$0^+$	0.00	0.5477 $N=3$					1.1819 $N=2$
$3^-$	6.13	0.4593 $N=2$	0.4393 $N=3$		0.4561 $N=2$		0.5020 $N=1$
$2^+$	6.92	0.8240 $N=4$	0.0707 $N=5$		0.1049 $N=4$		0.2933 $N=3$
$2^-$	8.87			0.3066 $N=3$		0.6411 $N=2$	
$4^+$	10.35	0.7855 $N=3$	0.3098 $N=4$		0.0632 $N=3$		0.1517 $N=2$

only, at a  $^6\text{Li}$  bombarding energy of 20 MeV the experiment was carried out with a polarized beam, and angular distributions of the vector analyzing powers were obtained. They were able to obtain a good fit to the cross section and analyzing power data using a cluster-folded  $^6\text{Li}+^{12}\text{C}$  spin-orbit potential.

Finally, there is the finite-range DWBA analysis of Drummer *et al.* [8], which analyses data for transfer to the 0.0-MeV  $0^+$  state of  $^{16}\text{O}$  using a 50-MeV polarized  $^6\text{Li}$  beam. A full set of analyzing powers was obtained and good fits to the data were obtained with both  $^6\text{Li}+^{12}\text{C}$  and  $d+^{16}\text{O}$  spin-orbit potentials included. It was found that the calculated analyzing powers were dominated by the  $d+^{16}\text{O}$  spin-orbit potential.

Overall, DWBA calculations have proved adequate to describe the shape of the  $^{12}\text{C}(^6\text{Li},d)^{16}\text{O}$  angular distributions when a number of the input parameters have been varied. These variations even within one analysis have made it difficult to extract meaningful information about the nature of the reaction, and also cast doubt on the use of this reaction to extract  $^{16}\text{O}\rightarrow\alpha+^{12}\text{C}$  spectroscopic factors. The calculations described below are able to obtain similar quality fits to data with one adjustable parameter (the strength of the real part of the cluster-folding model potential), the rest of the input being taken direct from the literature without any adjustment.

#### IV. THE CALCULATIONS

The goal of this work was to investigate the role of  $\alpha$  particle transfer from the excited states of the projectile and

target, and to assess their impact on the extraction of spectroscopic information. Consequently, all calculations were carried out using the code FRESKO [18], version FRXP.14, which can include these contributions to the direct one-step process. In order to perform these calculations, the following ingredients are required: some means of accurately describing the excitation of  $^6\text{Li}$  to its unbound resonant and non-resonant  $\alpha$ - $d$  continuum states, spectroscopic amplitudes (including their signs) for  $\alpha$  transfer via the ground and excited states, an unambiguous definition of the  $\alpha$ - $^{12}\text{C}$  wave functions (binding potential radius and number of radial nodes), the  $d+^{16}\text{O}$  potential in the exit channels, and coupling strengths (both nuclear and Coulomb) for inelastic excitations of  $^{12}\text{C}$  and  $^{16}\text{O}$ . The details of these ingredients used in the current work are described below.

We utilized the  $\alpha$ - $d$  cluster-folding (CF) model description of  $^6\text{Li}$  with the continuum-discretized coupled-channels (CDCC) [19] method to take account of resonant and non-resonant  $\alpha$ - $d$  breakup. The  $\alpha$ - $d$  continuum was discretized into a series of bins with respect to the momentum  $\hbar k$  of the  $\alpha$ - $d$  relative motion in a way similar to Rusek *et al.* [20]. The wave functions of these bins were normalized to unity, the radius limiting their range being set to 30 fm. The continuum model space was limited to values  $L=0,1,2$  of the  $\alpha$ - $d$  relative angular momentum and  $0.0\leq k\leq 0.75\text{ fm}^{-1}$  with  $\Delta k=0.25\text{ fm}^{-1}$ . The binning scheme was suitably modified in the presence of the  $L=2$  resonances in order to avoid double counting. The three  $L=2$  resonances were treated as bins of widths  $\Delta E=0.1, 2.0,$  and  $3.0\text{ MeV}$  for the 2.18-MeV  $3^+$ , 4.31-MeV  $2^+$ , and 5.7-MeV  $1^+$  states, re-

TABLE II. The  $d+^{16}\text{O}$  optical potential parameters used in the  $^{12}\text{C}(^6\text{Li},d)^{16}\text{O}$  calculations at  $^6\text{Li}$  bombarding energies of 34 and 50 MeV. Potential depths are in MeV and radius and diffuseness parameters in fm. The potential form is given by Eq. (2).

$E(^6\text{Li})$	$V_R$	$r_R$	$a_R$	$W_V$	$r_V$	$a_V$	$W_S$	$r_S$	$a_S$	$V_{\text{SO}}$	$r_{\text{SO}}$	$a_{\text{SO}}$	$W_{\text{SO}}$	$r_W$	$a_W$
34	89.3	0.99	0.95	9.5	1.65	0.3	4.1	2.25	0.3	1.0	0.40	0.27	1.75	1.15	0.35
50	89.3	0.99	0.95	7.3	2.10	0.3	3.125	2.25	0.3	2.25	0.90	0.27	1.75	1.15	0.35

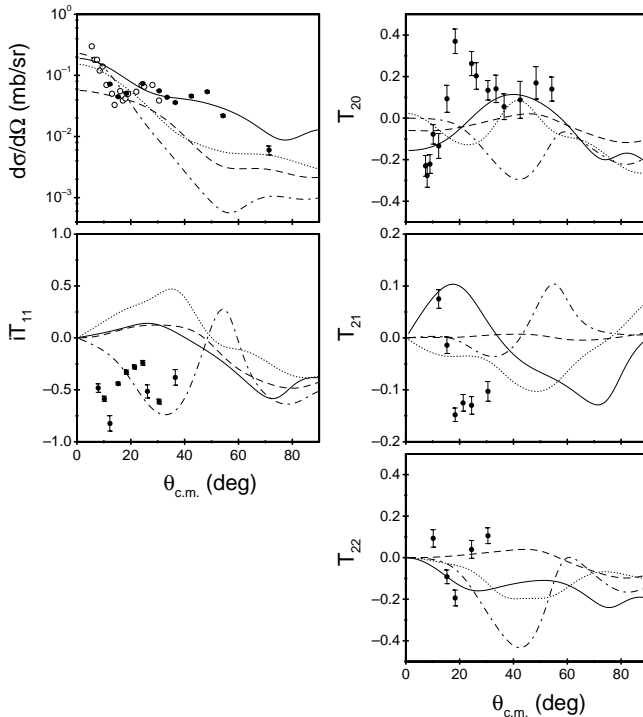


FIG. 2. Angular distributions for the  $^{12}\text{C}(^6\text{Li},d)^{16}\text{O}$  reaction leading to the 0.0-MeV  $0^+$  state of  $^{16}\text{O}$  for a  $^6\text{Li}$  bombarding energy of 34 MeV. The open circles denote the cross section data of Cunsolo *et al.* [7]. The dot-dashed curves denote the result of a calculation with direct  $\alpha$  transfer only, the dashed curves include transfer via the 4.44-MeV  $2^+$  state of  $^{12}\text{C}$ , the dotted curves include transfer via the three  $L=2$  resonances of  $^6\text{Li}$ , and the solid curves include couplings from the 0.0-MeV  $0^+$  state of  $^{16}\text{O}$  to the 6.92-MeV  $2^+$  and 6.13-MeV  $3^-$  states.

spectively. The  $\alpha$ - $d$  binding potential was as used by Kubo and Hirata [21].

The CF model requires  $\alpha + ^{12}\text{C}$  and  $d + ^{12}\text{C}$  optical model potentials at 2/3 and 1/3 of the  $^6\text{Li}$  beam energy, respectively. For the 34-MeV calculations, the nearest available potentials were the 27.2-MeV  $\alpha + ^{12}\text{C}$  of Nemets and Rudchik [22] and the 11.4-MeV  $d + ^{12}\text{C}$  of Guratzsch *et al.* [23]. In order to fit the elastic scattering data for 34-MeV  $^6\text{Li} + ^{12}\text{C}$  [24] with the full model space, the real and imaginary parts of the CF model potential had to be renormalized by factors of 0.5 and 0.6, respectively. For the 50-MeV calculations, the nearest available potentials were the 32.5-MeV  $\alpha + ^{12}\text{C}$  of Burdzik and Heyman [25] and the 15.9-MeV  $d + ^{12}\text{C}$  of Satchler [26]. In order to fit the 50-MeV  $^6\text{Li} + ^{12}\text{C}$  elastic scattering data [27], the real part of the CF model potential had to be renormalized by a factor of 0.6. Coupling to the 4.43-MeV  $2^+$  state of  $^{12}\text{C}$  was also included, using the rotational model. The  $0^+$  ground state and  $2^+$  excited state were considered to be the first two members of a  $K=0$  rotational band. The Coulomb coupling strength was taken from the measured  $B(E2;0^+ \rightarrow 2^+)$  [28] and the nuclear form factor was obtained by deforming the bare CF potential, with a nuclear deformation length derived from the  $B(E2)$  assuming a  $^{12}\text{C}$  radius of  $1.2 \times 12^{1/3}$  fm.

The following reaction paths were included in the full

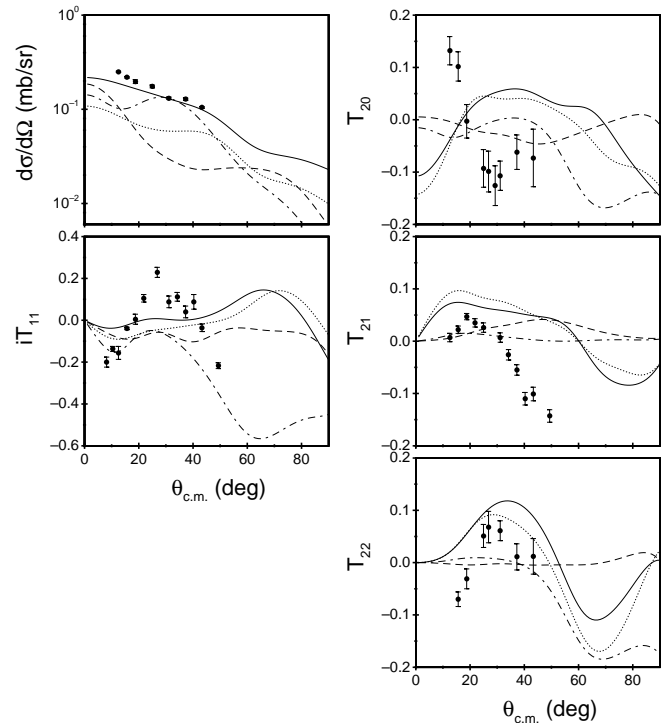


FIG. 3. Angular distributions for the  $^{12}\text{C}(^6\text{Li},d)^{16}\text{O}$  reaction leading to the 6.13-MeV  $3^-$  state of  $^{16}\text{O}$  for a  $^6\text{Li}$  bombarding energy of 34 MeV. The dot-dashed curves denote the result of a calculation with direct  $\alpha$  transfer only, the dashed curves include transfer via the 4.44-MeV  $2^+$  state of  $^{12}\text{C}$ , the dotted curves include transfer via the three  $L=2$  resonances of  $^6\text{Li}$ , and the solid curves include couplings from the 0.0-MeV  $0^+$  state of  $^{16}\text{O}$  to the 6.92-MeV  $2^+$  and 6.13-MeV  $3^-$  states.

calculations: transfer via the  $^6\text{Li}$  ground state and 2.18-MeV  $3^+$ , 4.31-MeV  $2^+$ , and 5.7-MeV  $1^+$   $L=2$  resonances of  $^6\text{Li}$ ; transfer via the  $^{12}\text{C}$   $0^+$  ground state and 4.43-MeV  $2^+$  state; and coupling between the  $0^+$  ground state and 6.13-MeV  $3^-$  and 6.92-MeV  $2^+$  states of  $^{16}\text{O}$  in the  $d + ^{16}\text{O}$  exit channel. Spectroscopic amplitudes for the four  $^6\text{Li}/d$  overlaps were set to 1.0, as we assumed a pure  $\alpha$ - $d$  cluster structure for  $^6\text{Li}$ . The  $D$ -state component of the  $^6\text{Li}$  ground state was ignored, as the work of Veal *et al.* [29] shows that it is very small, and it was found previously to have little influence on the  $^{12}\text{C}(^6\text{Li},d)$  transfer to the  $^{16}\text{O}$  ground state [8]. The  $\alpha$ - $d$  binding potential was as used in the CF model calculation and the three  $L=2$  resonances were treated as unbound resonance bins in the same way as for the CDCC calculation described above. The unbound component of the 10.35-MeV  $4^+$  state built on the  $^{12}\text{C}$   $0^+$  ground state was treated as a conventional bound state with a small (0.01 MeV) binding energy for the purposes of these calculations. Tests, where this component was treated as a narrow resonance, produced results that gave the same magnitude cross section as for the weak-binding approximation, but which exhibited spurious oscillations due to numerical solution problems associated with the long tail of the resonance wave function.

Spectroscopic amplitudes for the  $^{12}\text{C}(0^+)/^{16}\text{O}$  and  $^{12}\text{C}(2^+)/^{16}\text{O}$  overlaps were taken from the calculations of

Suzuki [30]. The results of these calculations are given as spectroscopic factors ( $C^2S$ ), which are unsigned, whereas FRESKO requires spectroscopic amplitudes  $\sqrt{C^2S}$  as input, which are signed. As we had no information as to the relative signs of the spectroscopic amplitudes, we adopted the simplest approach for the main calculations and took the same sign for all. The number of radial nodes was determined by the usual Talmi-Moshinsky relationship. The spectroscopic amplitudes and the number of radial nodes used in the present calculations are given in Table I.

The  $\alpha$ - $^{12}\text{C}$  binding potential was of Woods-Saxon form, with radius  $1.34 \times 12^{1/3}$  fm and diffuseness 0.65 fm, the depth being adjusted to give the correct binding energy in each case. As noted previously [8,21], there is some ambiguity as to the choice of binding potential radius for the  $\alpha + ^{12}\text{C}$  system. Many studies [5,6,21] have adopted a value consistent with the results of electron scattering, while others have chosen the value obtained from  $R = 1.25(4^{1/3} + 12^{1/3})$  fm [7]. For our main calculations, we have chosen to follow those studies that use a value consistent with electron scattering, with a radius similar to that used by Kubo and Hirata [21] and slightly larger than that adopted by Becchetti *et al.* [5,6].

The  $d + ^{16}\text{O}$  optical potential for the 34-MeV calculations was obtained from a fit to the elastic scattering data of Newman *et al.* [31], while that for the 50-MeV calculations was obtained by fitting the data of Hinterberger *et al.* [32]. As neither of these datasets contains analyzing powers, nor are these available at the appropriate deuteron bombarding energies, the spin-orbit components of the  $d + ^{16}\text{O}$  optical potentials were obtained from finite-range DWBA calculations that produced a simultaneous fit to the  $d + ^{16}\text{O}$  cross section data and the analyzing power data for the  $^{12}\text{C}(^6\text{Li}, d)$  transfer to the  $^{16}\text{O}$  ground state [14]. The form of the  $d + ^{16}\text{O}$  optical potentials was as follows:

$$V(r) = -V_R f(x_R) - i \left\{ W_V f(x_V) - 4W_S \frac{d}{dx_S} f(x_S) \right\} + 4 \frac{V_{SO}}{r} \frac{d}{dr} f(x_{SO}) \ell \cdot \mathbf{s} + 4i \frac{W_{SO}}{r} \frac{d}{dr} f(x_W) \ell \cdot \mathbf{s}, \quad (2)$$

where  $f(x_i) = (1 + \exp x_i)^{-1}$  and  $x_i = (r - r_i \times 12^{1/3})/a_i$ . The values of the parameters are given in Table II.

Coupling between the  $^{16}\text{O}$   $0^+$  ground state and 6.13-MeV  $3^-$  and 6.92-MeV  $2^+$  states were included using the vibrational model. The Coulomb coupling strengths were obtained from the measured  $B(E2; 0^+ \rightarrow 2^+)$  [28] and  $B(E3; 0^+ \rightarrow 3^-)$  [33] values. The nuclear form factors were obtained by deforming the  $d + ^{16}\text{O}$  optical potentials with deformation lengths obtained from the  $B(E2)$  and  $B(E3)$  values, assuming a  $^{16}\text{O}$  radius of  $1.2 \times 16^{1/3}$  fm. For the full calculations which included these couplings in the  $d + ^{16}\text{O}$  channel, the imaginary potential strengths were reduced to  $W_V = 7.3$  MeV and  $W_S = 3.125$  MeV for the 34-MeV calculation, and  $W_V = 5.0$  MeV and  $W_S = 2.3$  MeV for the 50-MeV

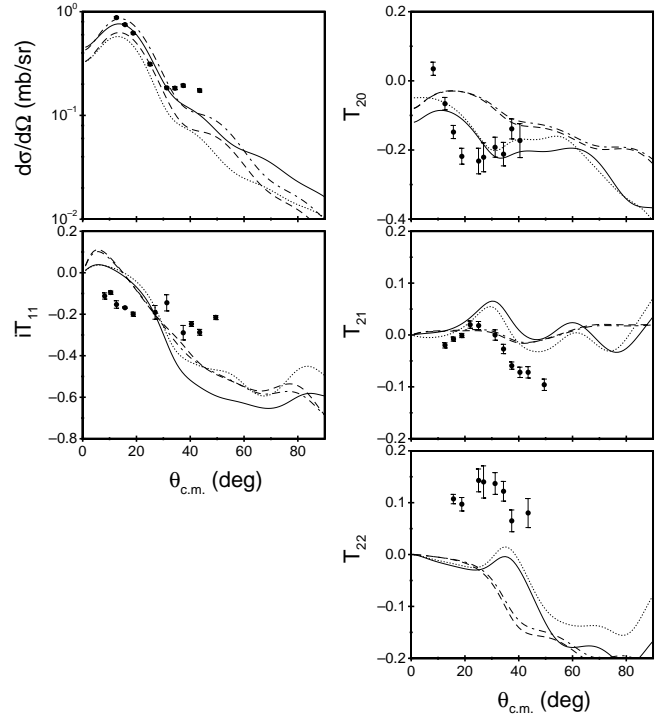


FIG. 4. Angular distributions for the  $^{12}\text{C}(^6\text{Li}, d)^{16}\text{O}$  reaction leading to the 6.92-MeV  $2^+$  state of  $^{16}\text{O}$  for a  $^6\text{Li}$  bombarding energy of 34 MeV. The dot-dashed curves denote the result of a calculation with direct  $\alpha$  transfer only, the dashed curves include transfer via the 4.44-MeV  $2^+$  state of  $^{12}\text{C}$ , the dotted curves include transfer via the three  $L=2$  resonances of  $^6\text{Li}$ , and the solid curves include couplings from the 0.0-MeV  $0^+$  state of  $^{16}\text{O}$  to the 6.92-MeV  $2^+$  and 6.13-MeV  $3^-$  states.

calculation in order to retain the fit to the elastic deuteron data of Newman *et al.* [31] and Hinterberger *et al.* [32], respectively.

As no couplings between the  $^{16}\text{O}$   $0^+$  ground state and either the  $^{16}\text{O}$  10.35-MeV  $4^+$  or 8.87-MeV  $2^-$  states were included, separate calculations were carried out for transfers to these states in order to save on computing time. As the effect of the transfer couplings on the elastic scattering was negligible in all cases, the results of these separate calculations should be identical to those that would have been obtained if transfers to the  $4^+$  and  $2^-$  states were included in the main calculations.

## V. RESULTS

In Figs. 2–11, we show the results of our calculations for the  $^{12}\text{C}(^6\text{Li}, d)^{16}\text{O}$  reaction leading to the 0.0-MeV  $0^+$ , 6.13-MeV  $3^-$ , 6.92-MeV  $2^+$ , 8.87-MeV  $2^-$ , and 10.35-MeV  $4^+$  states of  $^{16}\text{O}$  at  $^6\text{Li}$  bombarding energies of 34 and 50 MeV. In order to elucidate the contributions of the various multistep paths, we show four curves on each figure. The dot-dashed curves denote the results of calculations that include the full CDCC model space of  $^6\text{Li}$  plus coupling to the 4.44-MeV  $2^+$  state of  $^{12}\text{C}$ , but which only include direct  $\alpha$  transfer, with no multistep paths. The dashed curves indicate the results of calculations which include transfer via the  $^{12}\text{C}$

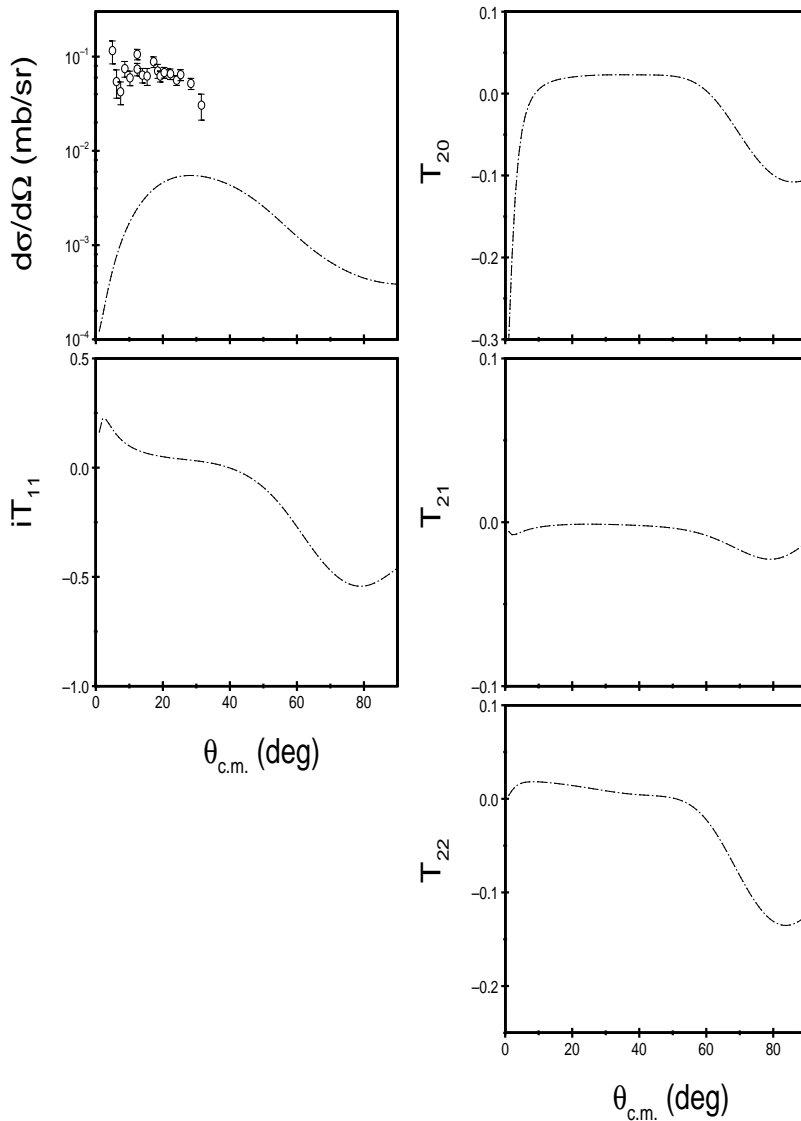


FIG. 5. Angular distributions for the  $^{12}\text{C}(^6\text{Li},d)^{16}\text{O}$  reaction leading to the 8.87-MeV  $2^-$  state of  $^{16}\text{O}$  at a  $^6\text{Li}$  bombarding energy of 34 MeV. The open circles denote the cross section data of Cunsolo *et al.* [7], the dashed curves denote the result of a calculation with transfer via the 4.44-MeV  $2^+$  state of  $^{12}\text{C}$ , and the dotted curves include transfer via the three  $L=2$  resonances of  $^6\text{Li}$ .

4.44-MeV  $2^+$  state in addition to the other couplings. The dotted curves denote the effect of adding transfers via the three  $L=2$  resonances of  $^6\text{Li}$ . Finally, the solid curves denote the results of the complete calculations, which add couplings between the 0.0-MeV  $0^+$  and 6.13-MeV  $3^-$ , and 6.92-MeV  $2^+$  states of  $^{16}\text{O}$  in the exit partition. As our calculations did not include any couplings within  $^{16}\text{O}$  leading to either the 8.87-MeV  $2^-$  or 10.35-MeV  $4^+$  states, the figures for these states do not exhibit solid curves. Also, as the 8.87-MeV un-natural parity  $2^-$  state of  $^{16}\text{O}$  cannot be formed by direct  $\alpha$  transfer via the  $0^+$  ground state of  $^{12}\text{C}$ , the figures for this state do not show dot-dashed curves.

Considering the 34-MeV data first, Figs. 2–6 show that the full calculations provide a reasonable description of the cross section angular distributions for transfer to the 0.0-MeV  $0^+$ , 6.13-MeV  $3^-$ , and 6.92 MeV- $2^+$  states. However, the analyzing powers for these states are rather poorly described. For the un-natural parity 8.87-MeV  $2^-$  state, previously considered to be populated solely by the compound nucleus mechanism [5–7], our calculation underpredicts the cross section data by approximately a factor of 10 (analyzing

power data were not obtained for this state for a  $^6\text{Li}$  bombarding energy of 34 MeV). The shape of the measured cross section angular distribution is also poorly described by the calculation. It will be noted that the addition of transfer via the three  $L=2$  resonances of  $^6\text{Li}$  has no effect on either the predicted cross section or analyzing powers for this state. For the 10.35-MeV  $4^+$  state the magnitude of the calculated cross section matches the data, but its shape is wrong, being peaked at forward angles while the data are relatively flat. The analyzing powers are again rather poorly described.

For a  $^6\text{Li}$  bombarding energy of 50 MeV, Figs. 7–11 show that at this energy the calculations are in worse agreement with the data than at 34 MeV. By contrast with the 34-MeV case, the description of the 0.0-MeV  $0^+$  and 6.13-MeV  $3^-$  cross section data by the full calculation is poor. The description of the 6.92-MeV  $2^+$  cross section is still reasonable, though not as good as that obtained at 34 MeV. For the 8.87-MeV  $2^-$  state, while the shape of the cross section angular distribution is rather better described than at 34 MeV, the magnitude of the calculated cross section is now a factor of approximately 70 times smaller than the measured

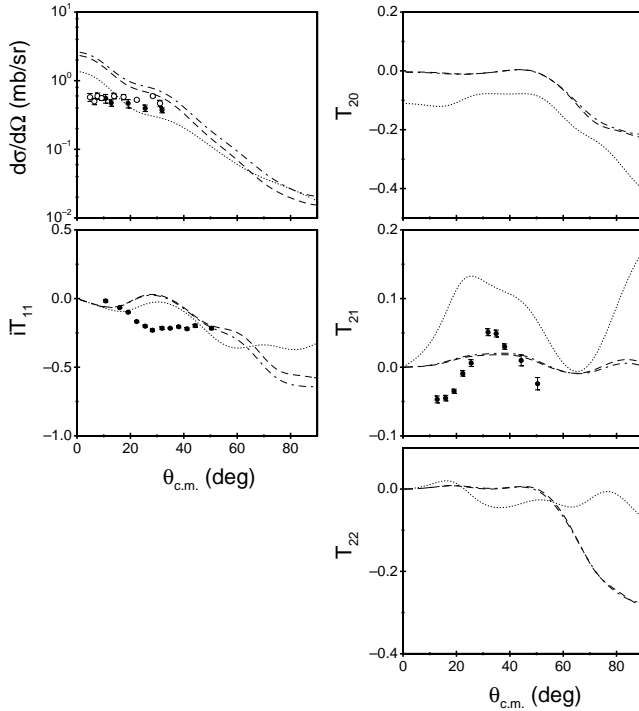


FIG. 6. Angular distributions for the  $^{12}\text{C}(^6\text{Li},d)^{16}\text{O}$  reaction leading to the 10.35-MeV  $4^+$  state of  $^{16}\text{O}$  at a  $^6\text{Li}$  bombarding energy of 34 MeV. The open circles denote the cross section data of Cunsolo *et al.* [7], the dot-dashed curves denote the result of a calculation with direct  $\alpha$  transfer only, the dashed curves include transfer via the 4.44-MeV  $2^+$  state of  $^{12}\text{C}$ , and the dotted curves include transfer via the three  $L=2$  resonances of  $^6\text{Li}$ .

one. Again, it will be noted that the addition of transfer via the  $L=2$  resonances of  $^6\text{Li}$  has no effect on the calculated cross section or analyzing powers for this state. Finally, the description of the 10.35-MeV  $4^+$  state cross section is similar to that obtained at 34 MeV, although the magnitude is now somewhat underpredicted. With a few exceptions, the analyzing powers for all states are again rather poorly described.

Before proceeding to a detailed discussion of the results of our calculations the question of the effect of the exit channel  $d+^{16}\text{O}$  spin-orbit potential on the calculated analyzing powers must be addressed. As there are no polarized deuteron scattering data available at suitable energies, the  $d+^{16}\text{O}$  spin-orbit potentials used in our analysis are poorly determined. Therefore, it is possible that the rather poor description of the  $^{12}\text{C}(^6\text{Li},d)^{16}\text{O}$  analyzing powers is merely due to lack of knowledge of the spin-orbit potentials. In Fig. 12 we compare the results of calculations for the  $^{12}\text{C}(^6\text{Li},d)$  transfer leading to the 6.92-MeV  $2^+$  state in  $^{16}\text{O}$  at a  $^6\text{Li}$  bombarding energy of 50 MeV using the full set of couplings with (solid curves) and without (dotted curves) a  $d+^{16}\text{O}$  spin-orbit potential included. As can be seen from the figure, the exit channel spin-orbit potential has considerable influence on the calculated analyzing powers. The same is true for transfers to the other states in  $^{16}\text{O}$  considered here (similar effects are observed at 34 MeV). Thus, the analyzing powers do not provide any useful extra information with

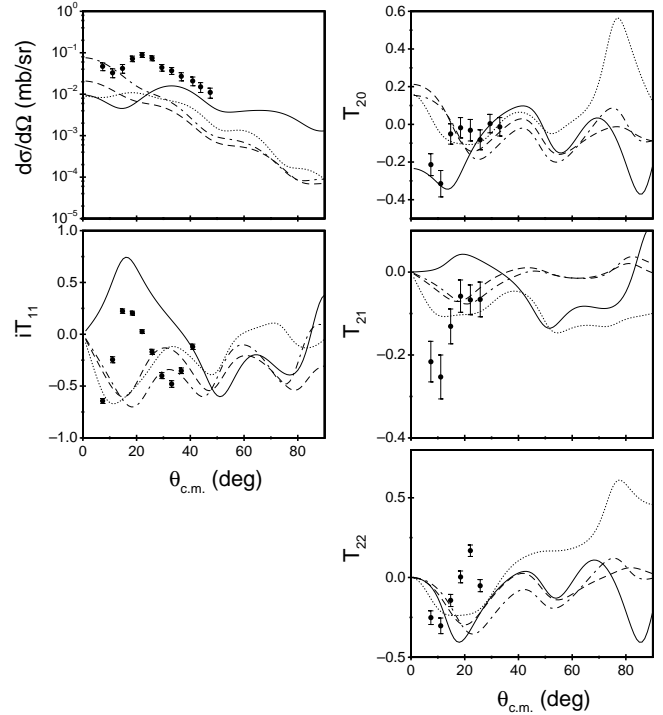


FIG. 7. Angular distributions for the  $^{12}\text{C}(^6\text{Li},d)^{16}\text{O}$  reaction leading to the 0.0-MeV  $0^+$  state of  $^{16}\text{O}$  for a  $^6\text{Li}$  bombarding energy of 50 MeV. The dot-dashed curves denote the result of a calculation with direct  $\alpha$  transfer only, the dashed curves include transfer via the 4.44-MeV  $2^+$  state of  $^{12}\text{C}$ , the dotted curves include transfer via the three  $L=2$  resonances of  $^6\text{Li}$ , and the solid curves include couplings from the 0.0-MeV  $0^+$  state of  $^{16}\text{O}$  to the 6.92-MeV  $2^+$  and 6.13-MeV  $3^-$  states.

which to test our calculations in this instance, as the calculated values are dominated by the effect of the  $d+^{16}\text{O}$  spin-orbit potential, which is not known with any.

Having thus established that the major influence on the calculated analyzing powers at both  $^6\text{Li}$  bombarding energies is the poorly determined  $d+^{16}\text{O}$  spin-orbit potential, we shall concentrate on the agreement between calculated and measured cross sections. As a general observation, we may note that the agreement between calculations and data is worse at 50 MeV than it is at 34 MeV, suggesting that there are processes not included in our calculations that become more important as the  $^6\text{Li}$  bombarding energy is increased. As compound nucleus contributions become less important with increasing bombarding energy [5], the poorer agreement at 50 MeV implies that multistep processes are increasing in importance as the bombarding energy is increased. This is further borne out by the angular momentum mismatches for each transfer at the two energies, given in Table III.

As Table III shows, the angular momentum mismatch at 50 MeV is significantly greater than at 34 MeV, further indicative of an increased importance of multistep processes as the  $^6\text{Li}$  bombarding energy is increased.

One may also note the importance of other multistep paths not considered in this work in the mechanism for populating the 8.87-MeV  $2^-$  state. As this is an un-natural parity state, it cannot be populated by direct  $\alpha$  transfer. As our

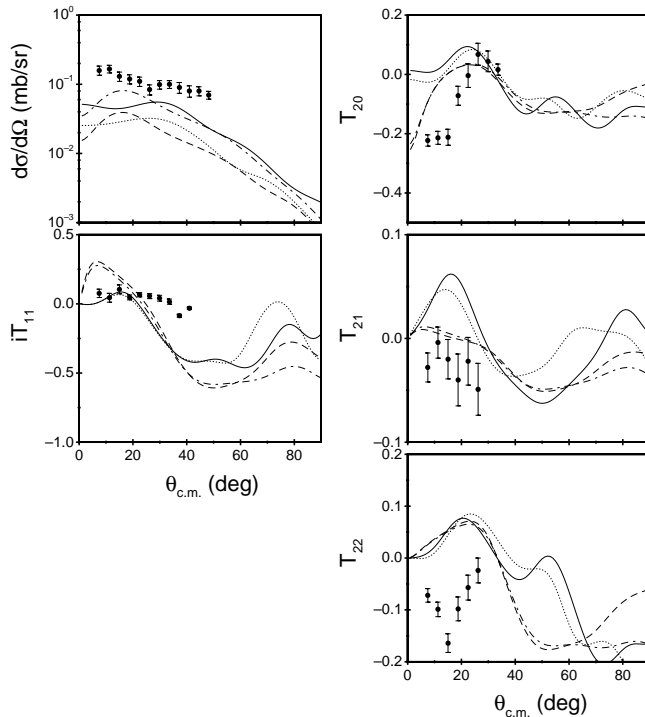


FIG. 8. Angular distributions for the  $^{12}\text{C}(^6\text{Li},d)^{16}\text{O}$  reaction leading to the 6.13-MeV  $3^-$  state of  $^{16}\text{O}$  for a  $^6\text{Li}$  bombarding energy of 50 MeV. The dot-dashed curves denote the result of a calculation with direct  $\alpha$  transfer only, the dashed curves include transfer via the 4.44-MeV  $2^+$  state of  $^{12}\text{C}$ , the dotted curves include transfer via the three  $L=2$  resonances of  $^6\text{Li}$ , and the solid curves include couplings from the 0.0-MeV  $0^+$  state of  $^{16}\text{O}$  to the 6.92-MeV  $2^+$  and 6.13-MeV  $3^-$  states.

calculations (which consider the multistep routes to this state via the  $^{12}\text{C}$  4.44-MeV  $2^+$  state) predict cross sections considerably smaller than the measured ones at both  $^6\text{Li}$  bombarding energies, it would be natural to assume that this state is largely populated via the compound nucleus method, as was done previously [5–7]. However, as noted above, the discrepancy between calculated and measured cross sections is significantly larger at 50 MeV than it is at 34 MeV. This difference suggests that the balance of the cross section strength may come from other multistep routes that we have not included in our calculations. Further evidence for this conclusion is provided by the measured vector analyzing power  $iT_{11}$  for the  $^{12}\text{C}(^6\text{Li},d)^{16}\text{O}_{2-}$  transfer at 50 MeV. The measured values of  $iT_{11}$  are significantly different from zero, ranging from  $\sim 0.5$  to  $-0.5$ . Compound nucleus processes are unable to produce large vector analyzing powers, thus the  $iT_{11}$  measurement is a strong indication that the discrepancy between the calculated and measured cross sections for the  $2^-$  state cannot be largely accounted for by compound nucleus contributions and must be due to multistep paths not included in the current calculations. Such paths might include transfer via the  $^{12}\text{C}$  9.64-MeV  $3^-$  state or transitions from other states in  $^{16}\text{O}$  to the 8.87-MeV  $2^-$  state. We did not include such couplings in our calculations due to a lack of definite values for the necessary spectroscopic amplitudes

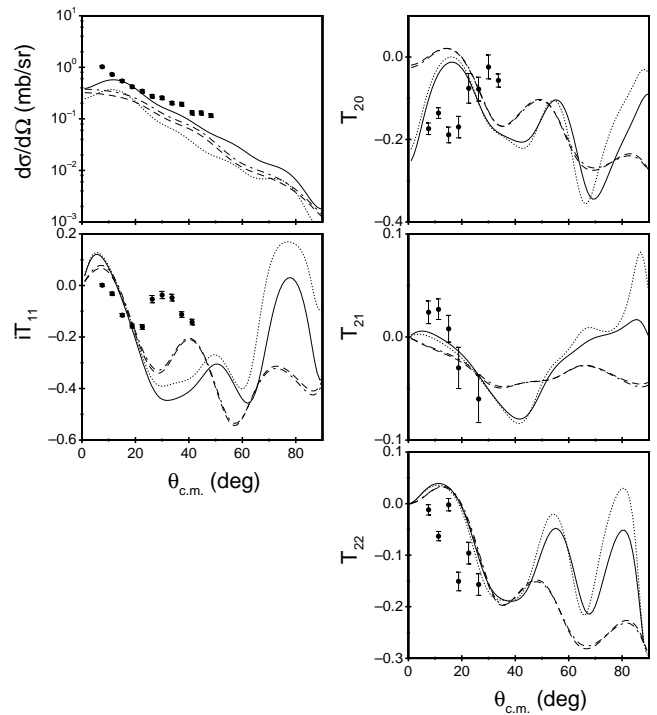


FIG. 9. Angular distributions for the  $^{12}\text{C}(^6\text{Li},d)^{16}\text{O}$  reaction leading to the 6.92-MeV  $2^+$  state of  $^{16}\text{O}$  for a  $^6\text{Li}$  bombarding energy of 50 MeV. The dot-dashed curves denote the result of a calculation with direct  $\alpha$  transfer only, the dashed curves include transfer via the 4.44-MeV  $2^+$  state of  $^{12}\text{C}$ , the dotted curves include transfer via the three  $L=2$  resonances of  $^6\text{Li}$ , and the solid curves include couplings from the 0.0-MeV  $0^+$  state of  $^{16}\text{O}$  to the 6.92-MeV  $2^+$  and 6.13-MeV  $3^-$  states.

and coupling strengths which would have made it difficult to draw worthwhile conclusions.

The inclusion of multistep transfer paths has a large effect on the  $^{12}\text{C}(^6\text{Li},d)$  transfers to the  $^{16}\text{O}$  0.0-MeV  $0^+$  and 6.13-MeV  $3^-$  states at both  $^6\text{Li}$  bombarding energies considered here. For transfer leading to the 6.92-MeV  $2^+$  and 10.35-MeV  $4^+$  states the effect of the multistep paths is much less pronounced, particularly so for the  $2^+$  state, so that these transfers might be reasonably accurately modeled as simple direct  $\alpha$  transfer only. However, this last statement needs some qualification, as there is the question of the effect of the signs of the spectroscopic amplitudes for the  $^{16}\text{O}/^{12}\text{C}$  overlap, which are not determined, and that of the radius of the  $\alpha$ - $^{12}\text{C}$  binding potential.

As stated above, there is some ambiguity in the choice of  $\alpha$ - $^{12}\text{C}$  binding potential radius. In the calculations presented here we used a Woods-Saxon well of radius  $1.34 \times 12^{1/3}$  fm. In order to test the effect of the value chosen for binding potential radius we repeated the calculations with a radius of  $1.25(4^{1/3} + 12^{1/3})$  fm, a value used previously in several DWBA analyses of the  $^{12}\text{C}(^6\text{Li},d)$  reaction. As might be expected, the general effect of this increase in binding potential radius is to increase the magnitude of the calculated cross sections, at both  $^6\text{Li}$  bombarding energies. However, it also alters the shapes of the cross sections, leading to somewhat more structured angular distributions. In general, the larger

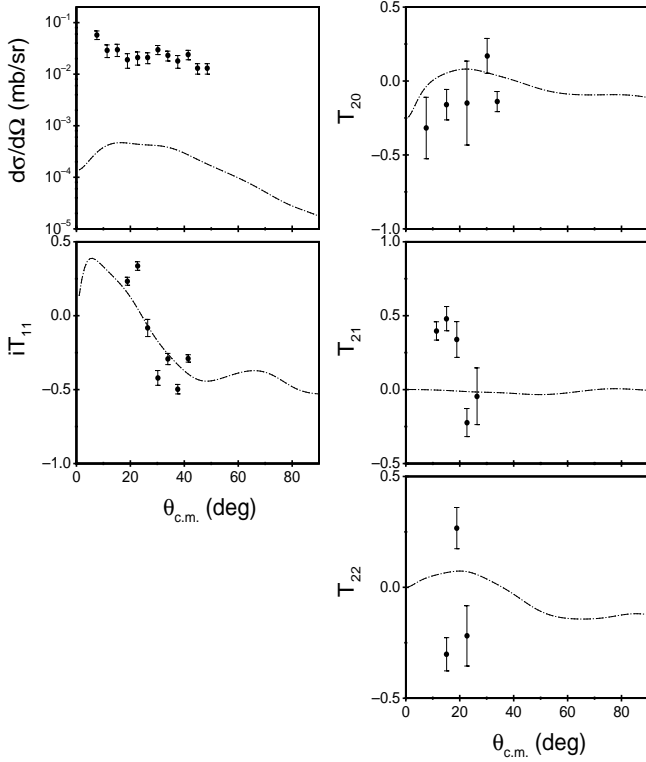


FIG. 10. Angular distributions for the  $^{12}\text{C}(^6\text{Li},d)^{16}\text{O}$  reaction leading to the 8.87-MeV  $2^-$  state of  $^{16}\text{O}$  at a  $^6\text{Li}$  bombarding energy of 50 MeV. The dashed curves denote the result of a calculation with transfer via the 4.44-MeV  $2^+$  state of  $^{12}\text{C}$ , and the dotted curves include transfer via the three  $L=2$  resonances of  $^6\text{Li}$ .

radius leads to overprediction of the magnitudes of the cross sections for transfer to the 6.13-MeV  $3^-$ , 6.92-MeV  $2^+$ , and 10.35-MeV  $4^+$  states, with the main effect on transfer to the 0.0-MeV  $0^+$  and 8.87-MeV  $2^-$  states begin to alter the shape of the cross section angular distributions. Importantly, the change in  $\alpha$ - $^{12}\text{C}$  binding potential radius does not affect the conclusion that transfer to the 6.92-MeV  $2^+$  and 10.35-MeV  $4^+$  states may be reasonably accurately described by a simple direct one-step  $\alpha$  transfer.

We also carried out an extensive series of test calculations investigating the effect of changing the signs of the  $^{16}\text{O}/^{12}\text{C}$  overlap spectroscopic amplitudes. The calculations of Suzuki [30] give spectroscopic *factors*, which are unsigned, rather than the signed spectroscopic *amplitudes* which are needed for coupled-reaction-channel calculations. In the calculations presented here, we adopted the simplest approach of keeping all  $^{16}\text{O}/^{12}\text{C}$  spectroscopic amplitudes positive. In our test calculations, we investigated the effect of giving the spectroscopic amplitudes for the  $^{16}\text{O}/^{12}\text{C}(2^+)$  overlaps negative signs while keeping those for the  $^{16}\text{O}/^{12}\text{C}(0^+)$  overlaps positive. The main effect of choosing negative signs for the  $^{16}\text{O}/^{12}\text{C}(2^+)$  overlap spectroscopic amplitudes for a particular  $^{16}\text{O}$  final state was to produce constructive interference between the direct  $\alpha$  transfer and the two-step  $\alpha$  transfer via the  $^{12}\text{C}$  4.44-MeV  $2^+$  state. The effect is larger at 34 MeV than at 50 MeV and is most noticeable for transfers leading to the 0.0-MeV  $0^+$  and 6.13-MeV  $3^-$  states of  $^{16}\text{O}$ . For

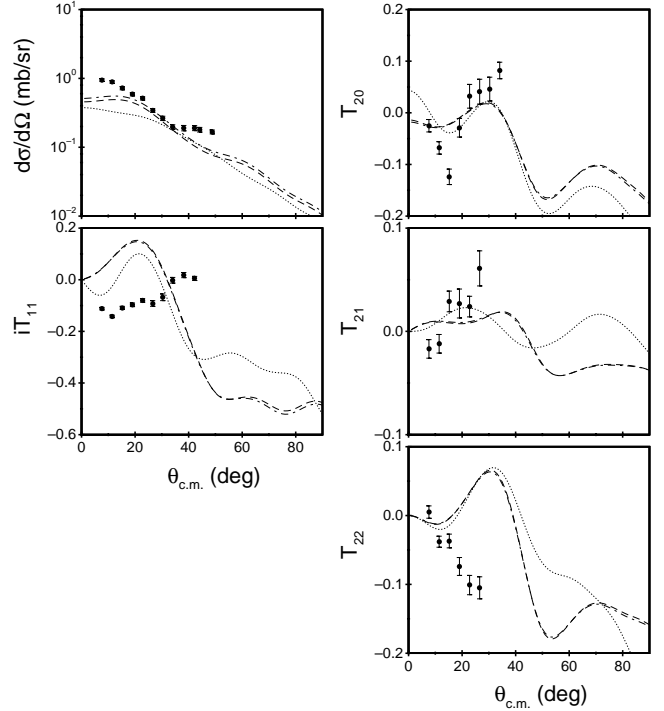


FIG. 11. Angular distributions for the  $^{12}\text{C}(^6\text{Li},d)^{16}\text{O}$  reaction leading to the 10.35-MeV  $4^+$  state of  $^{16}\text{O}$  at a  $^6\text{Li}$  bombarding energy of 50 MeV. The dot-dashed curves denote the result of a calculation with direct  $\alpha$  transfer only, the dashed curves include transfer via the 4.44-MeV  $2^+$  state of  $^{12}\text{C}$ , and the dotted curves include transfer via the three  $L=2$  resonances of  $^6\text{Li}$ .

transfers leading to the 6.92-MeV  $2^+$  and 10.35-MeV  $4^+$  states, the effect of changing the signs of the  $^{16}\text{O}/^{12}\text{C}(2^+)$  spectroscopic amplitudes at a  $^6\text{Li}$  bombarding energy of 34 MeV is sufficiently large to change the conclusion regarding the accuracy of their being described by simple direct  $\alpha$  transfer. The constructive interference of transfer via the  $^{12}\text{C}$  4.44-MeV  $2^+$  state produces significant effects on the cross section. However, at a  $^6\text{Li}$  bombarding energy of 50 MeV, the effect of changing the signs of the  $^{16}\text{O}/^{12}\text{C}(2^+)$  spectroscopic amplitudes is small enough that the previous conclusion about transfer to the 6.92-MeV  $2^+$  and 10.35-MeV  $4^+$   $^{16}\text{O}$  states still holds. They are reasonably well described by simple direct  $\alpha$  transfer. At both energies the best overall description of the data is obtained with all the spectroscopic amplitudes of positive sign.

## VI. CONCLUSIONS

In summary, we have presented here for the first time the results of extensive CRC calculations for the  $^{12}\text{C}(^6\text{Li},d)$  reaction at two  $^6\text{Li}$  bombarding energies, 34 and 50 MeV. We found that there were significant contributions from multi-step transfer processes at both energies for transfers leading to the 0.0-MeV  $0^+$  and 6.13-MeV  $3^-$  states of  $^{16}\text{O}$ . This conclusion is independent of the value chosen for the  $\alpha$ - $^{12}\text{C}$  binding potential radius or the relative signs of the  $^{16}\text{O}/^{12}\text{C}(0^+)$  and  $^{16}\text{O}/^{12}\text{C}(2^+)$  spectroscopic amplitudes. We also presented evidence suggesting that population of the

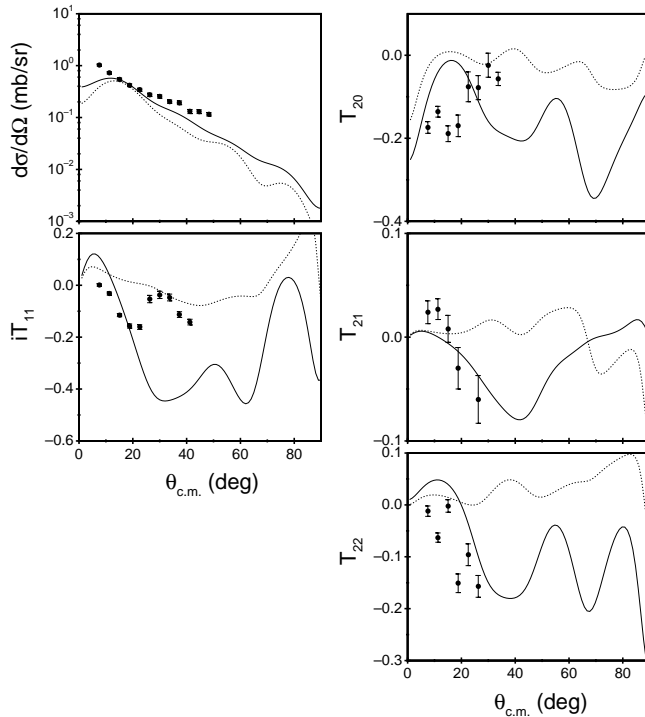


FIG. 12. Angular distributions for the  $^{12}\text{C}(^6\text{Li},d)^{16}\text{O}$  reaction leading to the 6.92-MeV  $2^+$  state of  $^{16}\text{O}$  for a  $^6\text{Li}$  bombarding energy of 50 MeV. The solid curves denote the result of the full calculation including a  $d + ^{16}\text{O}$  spin-orbit potential, while the dotted curves denote the result of a similar calculation without a  $d + ^{16}\text{O}$  spin-orbit potential.

un-natural parity 8.87-MeV  $2^-$  state of  $^{16}\text{O}$  may proceed in large part via multistep processes rather than via compound nucleus formation, as previously assumed. However, the present calculations greatly underpredict the observed cross section. We also found that for transfers leading to the 6.92-MeV  $2^+$  and 10.35-MeV  $4^+$  states of  $^{16}\text{O}$  multistep effects were less important, and that transfer to these states could be reasonably accurately modeled as simple direct  $\alpha$  transfer. Test calculations indicated that this conclusion is dependent on the relative signs of the  $^{16}\text{O}/^{12}\text{C}(0^+)$  and  $^{16}\text{O}/^{12}\text{C}(2^+)$  spectroscopic amplitudes for a  $^6\text{Li}$  bombarding energy of 34 MeV; at 50 MeV the effect of changing the relative signs of these amplitudes was sufficiently small to have no significant effect on the importance of multistep transfers. Clearly, if one wishes to obtain unambiguous results, a consistent cal-

TABLE III. Angular momentum mismatches for the  $^{12}\text{C}(^6\text{Li},d)^{16}\text{O}$  transfers considered in this work.

Final state in $^{16}\text{O}$	Angular momentum mismatch ( $\hbar$ )	
	34 MeV	50 MeV
0.00-MeV $0^+$	2.5	3.8
6.13-MeV $3^-$	3.5	4.6
6.92-MeV $2^+$	3.6	4.7
8.87-MeV $2^-$	3.9	4.9
10.35-MeV $4^+$	4.2	5.2

ulation of the spectroscopic amplitudes *with their signs* is required, along with a consistent set of  $\alpha + ^{12}\text{C}$  bound state wave functions. However, our results do unambiguously show that the DWBA is inadequate to describe the  $^{12}\text{C}(^6\text{Li},d)$  reaction leading to the 0.0-MeV  $0^+$  and 6.13-MeV  $3^-$  states of  $^{16}\text{O}$ , and thus that the asymptotic normalization coefficient method cannot be applied to these transitions.

It was also found that all the analyzing powers for the  $^{12}\text{C}(^6\text{Li},d)^{16}\text{O}$  reaction are dominated by the  $d$  spin-orbit potential. Yamaya *et al.* [34] found a similar situation for the  $^{12}\text{C}(^6\text{Li},d)^{16}\text{O}$  reaction, where the dominant influence on the vector analyzing power was the entrance channel  $d$  spin-orbit potential. Thus, in the case of the  $^{12}\text{C}(^6\text{Li},d)^{16}\text{O}$  reaction the analyzing powers unfortunately do not provide us with useful extra information with which to test our calculations.

With the current interest in transfer reactions involving radioactive beams, for both spectroscopic and astrophysical studies, the calculations presented here demonstrate that if one wishes to go beyond simple DWBA analyses that attempt to extract  $\alpha$  spectroscopic factors from  $(^6\text{Li},d)$  reactions (albeit in inverse kinematics), a considerable amount of nuclear structure information will be required. This information, of necessity, has to be obtained from structure calculations. Therefore, any meaningful CCBA/CRC analysis will require a consistent set of spectroscopic amplitudes (with the appropriate signs) plus  $B(E2)$  etc. values for the coupling strengths in the “target” nucleus (i.e., the radioactive nuclide comprising the beam in an inverse kinematics setup).

#### ACKNOWLEDGMENTS

This work was supported by the U.S. National Science Foundation, the U.S. Department of Energy, the State of Florida, and NATO, Grant No. PST.CLG.978953.

- [1] D.P. Balamuth, Phys. Rev. C **8**, 1185 (1973).
- [2] P.T. Debevec, H.T. Fortune, R.E. Segel, and J.F. Tonn, Phys. Rev. C **9**, 2451 (1974).
- [3] K.W. Kemper and T.R. Ophel, Aust. J. Phys. **33**, 197 (1980).
- [4] C.W. Glover and K.W. Kemper, Nucl. Phys. **A366**, 469 (1981).
- [5] F.D. Becchetti, J. Jänecke, and C.E. Thorn, Nucl. Phys. **A305**, 313 (1978).
- [6] F.D. Becchetti, D. Overway, J. Jänecke, and W.W. Jacobs,

Nucl. Phys. **A344**, 336 (1980).

- [7] A. Cunsolo, A. Foti, G. Pappalardo, G. Raciti, and N. Saunier, Phys. Rev. C **18**, 856 (1978).
- [8] T.L. Drummer, E.E. Bartosz, P.D. Cathers, M. Fauerbach, K.W. Kemper, E.G. Myers, and K. Rusek, Phys. Rev. C **59**, 2574 (1999).
- [9] K. Langanke and M. Wiescher, Rep. Prog. Phys. **64**, 1657 (2001).

- [10] A.M. Mukhamedzhanov *et al.*, Phys. Rev. C **56**, 1302 (1997).
- [11] F.M. Nunes and A.M. Mukhamedzhanov, Phys. Rev. C **64**, 062801(R) (2001).
- [12] E.G. Myers, A.J. Mendez, B.G. Schmidt, and K.W. Kemper, Nucl. Instrum. Methods Phys. Res. B **56/57**, 1156 (1991); E.G. Myers, A.J. Mendez, B.G. Schmidt, K.W. Kemper, P.L. Kerr, and E.L. Reber, *ibid.* **79**, 701 (1993).
- [13] A.J. Mendez, E.G. Myers, K.W. Kemper, P.L. Kerr, E.L. Reber, and B.G. Schmidt, Nucl. Instrum. Methods Phys. Res. A **329**, 37 (1993).
- [14] T. L. Drummer, Ph.D. thesis, Florida State University, 1998.
- [15] B. Apagyí and T. Vertse, Phys. Rev. C **21**, 779 (1980).
- [16] A. Insolia, M. Baldo, F. Catara, and A. Vitturi, Z. Phys. A **301**, 209 (1981).
- [17] M. Makowska-Rzeszutko, P. Egelhof, D. Kassen, E. Steffens, W. Weiss, D. Fick, W. Dreves, K.-I. Kubo, and T. Suzuki, Phys. Lett. **74B**, 187 (1978).
- [18] I.J. Thompson, Comput. Phys. Rep. **7**, 167 (1988).
- [19] Y. Sakuragi, M. Yahiro, and M. Kamimura, Prog. Theor. Phys. Suppl. **89**, 136 (1986).
- [20] K. Rusek, P.V. Green, P.L. Kerr, and K.W. Kemper, Phys. Rev. C **56**, 1895 (1997).
- [21] K.-I. Kubo and M. Hirata, Nucl. Phys. **A187**, 186 (1972).
- [22] O.F. Nemets and A.T. Rudchik, Sov. J. Nucl. Phys. **4**, 694 (1967).
- [23] H. Guratzsch, J. Slotta, and G. Stiller, Nucl. Phys. **A140**, 129 (1970).
- [24] E. L. Reber and K. W. Kemper (unpublished).
- [25] G.F. Burdzik and G. Heyman, Nucl. Phys. **A185**, 509 (1972).
- [26] G.R. Satchler, Nucl. Phys. **85**, 273 (1966).
- [27] P.L. Kerr, K.W. Kemper, P.V. Green, K. Mohajeri, E.G. Myers, D. Robson, and B.G. Schmidt, Phys. Rev. C **52**, 1924 (1995).
- [28] S. Raman, At. Data Nucl. Data Tables **42**, 1 (1989).
- [29] K.D. Veal *et al.*, Phys. Rev. Lett. **81**, 1187 (1998).
- [30] Y. Suzuki, Prog. Theor. Phys. **55**, 1751 (1976).
- [31] E. Newman, L.C. Becker, B.M. Preedom, and J.C. Hiebert, Nucl. Phys. **A100**, 225 (1967).
- [32] F. Hinterberger, G. Mairle, U. Schmidt-Rohr, G.J. Wagner, and P. Turek, Nucl. Phys. **A111**, 265 (1968).
- [33] R.H. Spear, At. Data Nucl. Data Tables **42**, 55 (1989).
- [34] T. Yamaya, J.I. Hirota, K. Takimoto, S. Shimoura, A. Sakaguchi, S. Kubono, M. Sugitani, S. Kato, T. Suehiro, and M. Fukada, Phys. Rev. C **34**, 2369 (1986).